

EFFECTS OF THALLIUM SALTS ON NEURONAL MITOCHONDRIA IN ORGANOTYPIC CORD-GANGLIA-MUSCLE COMBINATION CULTURES

PETER S. SPENCER, EDITH R. PETERSON,
RICARDO MADRID A., and CEDRIC S. RAINE

From the Department of Pathology (Neuropathology), the Saul R. Korey Department of Neurology, and the Rose F. Kennedy Center for Research in Mental Retardation and Human Development, Albert Einstein College of Medicine, Bronx, New York 10461

ABSTRACT

A functionally coupled organotypic complex of cultured dorsal root ganglia, spinal cord peripheral nerve, and muscle has been employed in an experimental approach to the investigation of the neurotoxic effects of thallium. Selected cultures, grown for up to 12 wk in vitro, were exposed to thallosalts for periods ranging up to 4 days. Cytopathic effects were first detected after 2 h of exposure with the appearance of considerably enlarged mitochondria in axons of peripheral nerve fibers. With time, the matrix space of these mitochondria became progressively swollen, transforming the organelle into an axonal vacuole bounded by the original outer mitochondrial membrane. Coalescence of adjacent axonal vacuoles produced massive internal axon compartments, the membranes of which were shown by electron microprobe mass spectrometry to have an affinity for thallium. Other axoplasmic components were displaced within a distended but intact axolemma. The resultant fiber swelling caused myelin retraction from nodes of Ranvier but no degeneration. Impulses could still propagate along the nerve fibers throughout the time course of the experiment. Comparable, but less severe changes were seen in dorsal root ganglion neurons and in central nerve fibers. Other cell types showed no mitochondrial change. It is uncertain how these findings relate to the neurotoxic effects of thallium in vivo, but a sensitivity of the nerve cell and especially its axon to thallosalts is indicated.

INTRODUCTION

Thallium is a heavy metal which exists as monovalent and trivalent ionic species (1). Considerable interest has centered on the ability of monovalent thallosalts (Tl^+) to mimic the biologic action of potassium ions (K^+). This has been attributed to the inability of cell membranes to distinguish between Tl^+ and K^+ , possibly because of similar ionic charge and crystal radius (2-5). Numerous studies have indicated that the Tl^+ competes for

the K^+ site in membrane transport systems which utilize (Na^+ , K^+)-dependent ATPase. Active transport, employing the substituted enzyme (Na^+ , Tl^+)-ATPase (2, 6), has been thought to account for the movement of Tl^+ across membranes derived from skin (7, 8), eye (4, 5), erythrocyte (9), kidney (2, 10), muscle (11-13), and brain (14).

The toxic effects of thallium in man and animals have also received considerable attention.

The use of thallium salts as human depilatory agents has been discontinued, so only rare cases of human toxicity occur after accidental or homicidal ingestion. Clinical signs of intoxication include diarrhea, alopecia, cataract, peripheral nervous system (PNS) dysfunction, and eventually death (7, 15–21). Today, thallosulfate is widely employed as a rodenticide (22). Experimentally intoxicated rats show mitochondrial changes in liver, kidney, intestine, and brain tissues (19).

Peterson and Murray, in a light microscope study of organized PNS tissue *in vitro* (23), demonstrated the formation of axonal vacuoles in peripheral nerve fibers exposed to thallium salts. The present study has examined the ultrastructural changes in nerve and muscle tissue exposed to monovalent thallium salts *in vitro* and attempts to identify their site of action. For this investigation, we have employed the recently developed organotypic cultures of cord-ganglia, functionally coupled to muscle tissue *in vitro* (25, 26).

MATERIALS AND METHODS

Résumé of Tissue Culture Techniques

Cross sections of fetal mouse spinal cord, 14 days *in utero*, with meningeal covering and attached dorsal root ganglia, were explanted singly on collagen-coated cover slips (27). Explants were provided with a drop of nutrient fluid and sealed into Maximow slide assemblies. The nutrient fluid consisted of Eagle's minimum essential medium with glutamine (53%), human placental serum (33%), chick embryo extract (10%), 6 mg/ml glucose, and 1.2 $\mu\text{g}/\text{ml}$ Achromycin with ascorbic acid. Cultures were incubated at 34°–35°C as lying drops. After 4 days, 3–6 mm lengths of teased skeletal muscle fibers from adult rats were positioned close to the zone of neuritic outgrowth. Cultures were maintained for 50–90 days *in vitro* with replacement of the nutrient fluid twice a week. Full details of the maintenance and growth of cord-ganglia-muscle preparations have been described elsewhere (25).

Intoxication

Well-myelinated cord-ganglia-muscle cultures were exposed to nutrient fluid containing Tl^+ in the form of either 10 $\mu\text{g}/\text{ml}$ thallosulfate ($\text{CH}_3\text{COO}\text{Tl}$) or 5–10 $\mu\text{g}/\text{ml}$ thallosulfate (Tl_2SO_4), i.e., $1\text{--}2 \times 10^{-5}$ M. Cultures were observed daily and selected preparations photographed by bright-field microscopy. During the intoxication period, electrophysiologic studies of intoxicated sister cultures were carried out; the results will be presented in detail

elsewhere¹ (for details of the techniques, see 28 and 29).

Preparation for Microscopy

Combination cultures treated with thallium salts were sampled after 2, 4, 8, and 12 h, and daily for 4 days. Four unintoxicated sister cultures were used as controls. A total of 22 cultures was sampled.

Cultures, attached to their collagen-coated coverslips, were immersed in cold phosphate-buffered 2.5% glutaraldehyde (pH 7.3) for 1 h, followed by 1 h in phosphate-buffered 1% osmium tetroxide at pH 7.3. Three cultures were not osmicated. Dehydration was achieved by 5-min immersions in a graded series of ethanol. Cultures were removed from cover slips while in 70% ethanol. After immersions in propylene oxide (2×10 min), the cultures were embedded horizontally in Epon, and incubated at 35°, 45°, and 60°C over a 48 h period (30).

Epon-embedded cultures were oriented to section either cord, dorsal root and associated ganglion cells, or terminal motor nerve fibers and muscle tissue. The position of the cut surface was continuously monitored by examination of 1 μm sections stained with toluidine blue. Suitable areas were photographed with a Zeiss photo microscope.

Thin sections were cut from selected areas of the culture using an LKB Ultratome III. Sections were stained with uranyl acetate and lead citrate, and examined in a Siemens 101 electron microscope.

Detection of Thallium

UNSTAINED SECTIONS: Thallium has an atomic number of 81. Thus, deposition of thallium in tissue sections would be detected as an electron-opaque precipitate (1, 2). Thin unstained sections of unsmicated and osmicated tissue were, therefore, used for the ultrastructural localization of electron-opaque deposits in intoxicated cultures, using sections from unexposed cultures as controls.

ELECTRON MICROPROBE ANALYSIS: Electron-opaque precipitates, located in thin (ca. 50 nm) or semithin (ca. 200 nm) sections of osmicated tissue, were also examined in a Philips 300 electron microscope equipped with an Edax microprobe element detector and graphic read-out (Edax International Inc.). The peak pattern produced by thallium atoms was calibrated using a pure sample of thallic oxide. In tissue sections, the detection of characteristic K_{α} (2.30 Å) and $K_{\beta 1}$ (10.25 Å) peaks was considered sufficient evidence to indicate the presence of thallium. An AEI EMMA 4 quantitative analytical electron microprobe analyzer was used to estimate the

¹Crain, S. M., and E. R. Peterson. In preparation.

relative concentration of osmium and thallium in areas where both heavy metals could be detected.

RESULTS

Unexposed Cultures

LIVING EXPLANT: In the cord-ganglia culture, there is coordinated development and differ-

entiation of both the central nervous system (CNS) and PNS complex (31). Onset and development in vitro of complex bioelectric activity in the spinal cord (29) correlates with the appearance and elaboration of synapses (32). Myelination of CNS fibers begins at about 7 days in vitro. A transition from CNS myelin to peripheral-type myelin occurs at the meningeal boundary of the spinal cord,

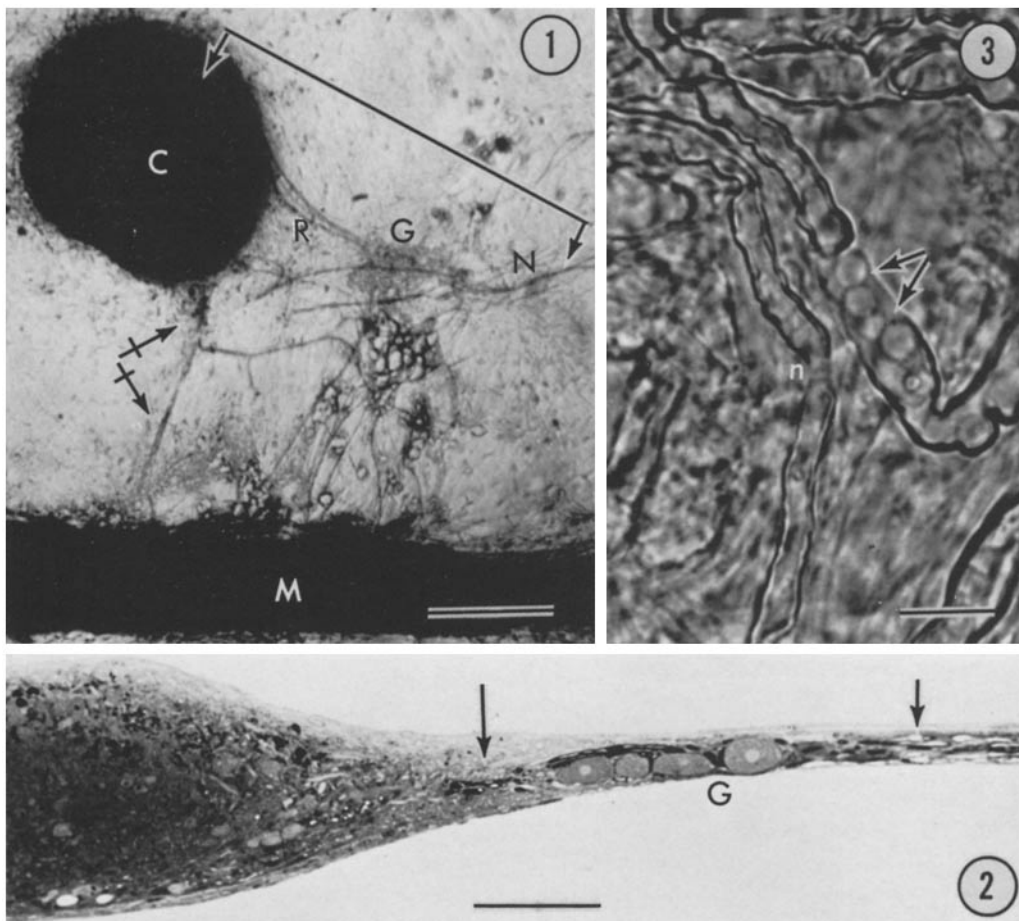
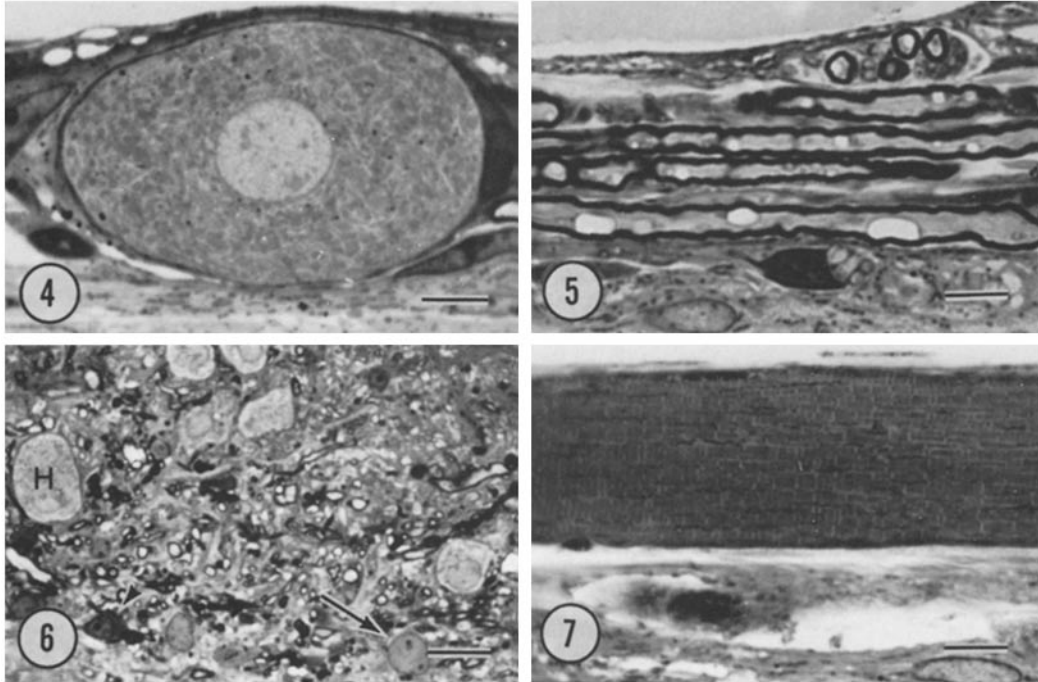


FIGURE 1 Light micrograph of a portion of a combination culture composed of functionally coupled peripheral nerve fibers (*N*), dorsal root ganglion cells (*G*), dorsal root (*R*), spinal cord (*C*), and muscle (*M*) tissue. Ventral root and motor PNS fibers are indicated by crossed arrows. These fibers traverse a surface growth of meningeal tissue which, in some areas, appears reticulated. Arrowed line indicates the plane of section which is illustrated in Fig. 2. Holme's silver stain. Bar, 500 μm . $\times 32$.

FIGURE 2 1 μm section of fixed tissue cut along a similar plane to that indicated by the line in Fig. 1. PNS fibers are visible (arrows) on either side of the dorsal root ganglion cells (*G*). These fibers enter the cord (left). Bar, 100 μm . $\times 160$.

FIGURE 3 Small vacuoles (arrows) are visible at a node of Ranvier of a PNS fiber after 24–48 h of exposure to thallosulfate. Local fiber swelling has caused the myelin to retract from the normal nodal position, seen on an adjacent unaffected fiber (*n*). Living culture. Bar, 25 μm . $\times 680$.



FIGURES 4-7 1 μ m Epon sections stained with toluidine blue.

FIGURE 4 A dorsal root ganglion cell shows an absence of visible changes after 48 h of exposure to thal-
lous sulfate. Bar, 10 μ m. \times 800.

FIGURE 5 Adjacent PNS fibers display isolated circular and oval axonal vacuoles after a similar exposure.
Bar, 10 μ m. \times 800.

FIGURE 6 Cord tissue containing CNS fibers (sometimes seen to be vacuolated at higher magnification),
neuron (H), astroglial cell (arrow), and oligodendroglial cell (arrowhead). 24 h of exposure to thal-
lous sulfate. Bar, 25 μ m. \times 310.

FIGURE 7 Skeletal muscle tissue appears unchanged after 1 wk of exposure to thal-
lous sulfate. Bar, 10 μ m. \times 800.

where dorsal and ventral roots may be clearly defined. PNS myelination proceeds gradually over a period of several weeks. The concurrent differentiation of CNS and PNS elements is essential to the development and function of an organotypic neuromuscular model. Adult skeletal muscle, incorporated into this system, regenerates and differentiates. Muscle maturation and prolonged maintenance are dependent upon innervation *in vitro*, as *in vivo*. Maturation of motor end plate structures proceeds during weeks *in vitro*, as shown by light microscopy (25) and electron microscopy (26). By 50 days *in vitro*, the shortest period selected for exposure to thallium salts, the total CNS-PNS-muscle complex is well differentiated and stable (Fig. 1).

MICROSCOPY OF EMBEDDED TISSUE: Representative portions of dorsal root ganglion cells, dorsal root fibers, and spinal cord were seen in 1 μ m sections (Fig. 2) cut along the plane indicated in Fig. 1. Reorientation of the tissue block was required for the sampling of terminal PNS motor fibers and muscle fibers. PNS fibers grown *in vitro* possess smaller diameters and shorter internodes compared with their *in vivo* counterparts. The organotypic nature and fine structure of explanted (rat) PNS tissue grown *in vitro* was the subject of a previous report (33). Few differences were noted in the PNS portions, derived from explanted mouse tissue, of our CNS-PNS-muscle combination cultures. PNS motor fibers lose their myelin, but not their Schwann cell ensheathment, as they ap-

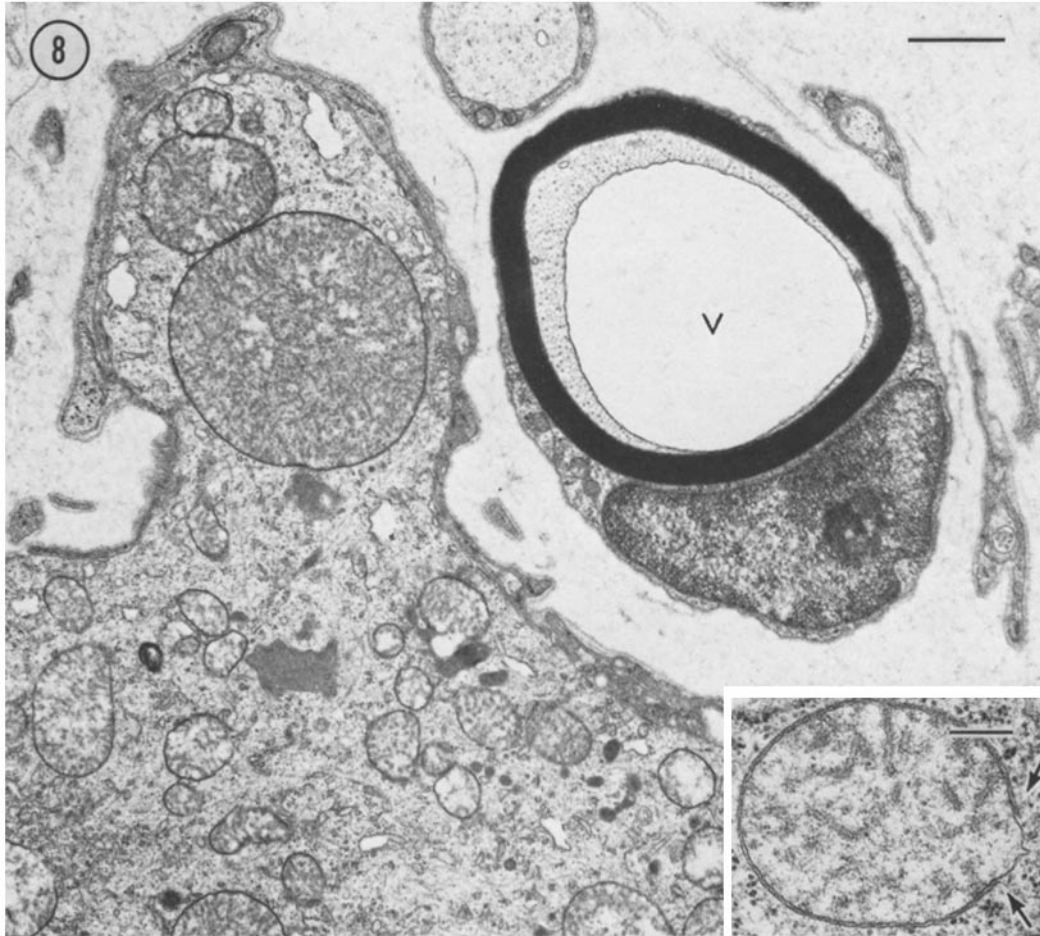


FIGURE 8 This electron micrograph illustrates a dorsal root ganglion cell containing enlarged perikaryal mitochondria. One mitochondrion, within a cytoplasmic protrusion, has a diameter of $2.6 \mu\text{m}$, similar in size to the vacuole (*V*) in an adjacent PNS fiber. 48 h of exposure to thallos sulfate. Bar, $1 \mu\text{m}$. *Inset* shows an enlarged perikaryal mitochondrion with a ruptured outer membrane (arrows) and poorly defined cristae. 1 wk exposure. Bar, $0.25 \mu\text{m}$. $\times 13,000$. *Inset*, $\times 30,000$.

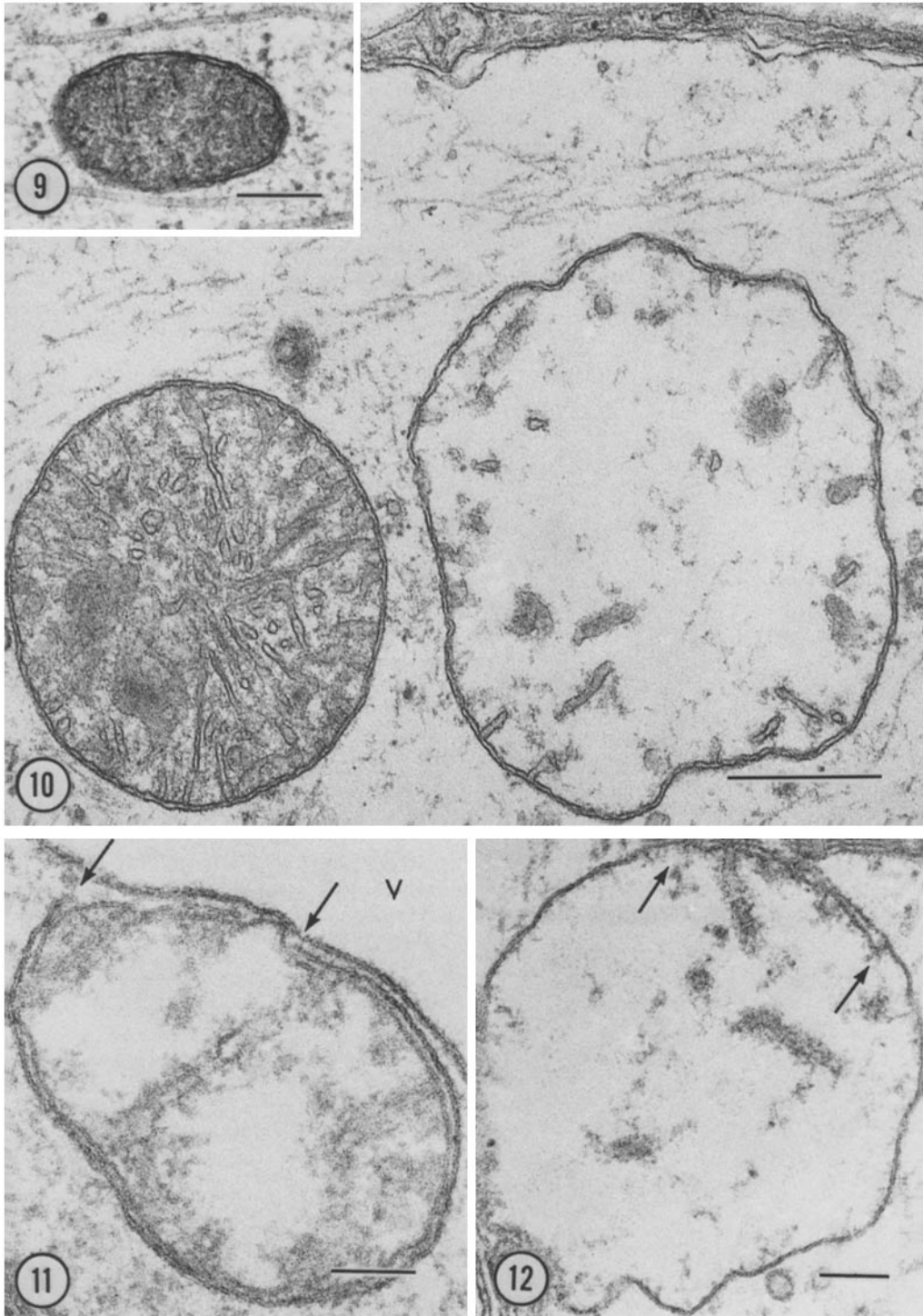
proach the muscle tissue which they innervate. The development and ultrastructure of neuromuscular junctions in this system has been previously studied (25, 26).

The spinal cord portion of the explant contained CNS myelinated fibers except where PNS fibers entered from the dorsal roots. Large neurons, the *in vitro* counterparts of anterior horn cells, were located deep within the cord explant. Other aspects of the organization of CNS tissue *in vitro* have been reviewed elsewhere (34).

Cultures Exposed to Thallos Salts

LIVING EXPLANT: 24 h exposure to thallos salts caused the formation of vacuoles in PNS fibers

of both dorsal roots and their distal outgrowths. These vacuoles appeared to be directly related to the axon and, in myelinated fibers, frequently originated close to nodes of Ranvier (Fig. 3). Longer exposure led to increased vacuolation, progressive fiber distortion, and juxtanyl retraction of myelin. Preliminary electrophysiologic tests after 4 days of exposure to $10 \mu\text{g/ml}$ thallos sulfate have indicated that local cord stimuli could still trigger complex cord discharges which propagated through peripheral axons and initiated characteristic contractions in the associated muscle tissue¹. This has demonstrated maintenance of bioelectric properties of at least major components of the cord synaptic networks, motor axons, and neu-



romuscular junctions, despite the presence of pronounced morphologic changes in nerve fibers, including presynaptic terminals.

The response of altered axons to withdrawal of the thallos salt from the nutrient fluid appears to be complex. While less affected fibers are able to recover gradually after early removal of thallium (23), more severely damaged fibers reacted in a complex and variable way which is presently under examination.

LIGHT MICROSCOPY OF EMBEDDED TISSUE: After 8–24 h of exposure, dorsal root ganglion cells showed no change (Fig. 4) but discrete vacuoles were visible in their axons (Fig. 5). The number of PNS fibers affected and the number of axonal vacuoles increased with continued exposure. Axonal vacuolation was difficult to detect in CNS fibers by light microscopy (Fig. 6). Muscle tissue displayed few changes even after a prolonged exposure (Fig. 7).

ELECTRON MICROSCOPY: Dorsal root ganglion neurons often contained large numbers of mitochondria, some of which were considerably enlarged and which possessed abundant cristae and a granular matrix space (Fig. 8). Outer mitochondrial membranes were sometimes ruptured (Fig. 8, inset). The endoplasmic reticulum, Golgi apparatus, and other cytoplasmic organelles were relatively unaffected.

The vacuoles seen in axons of PNS fibers were closely examined by electron microscopy in dorsal roots. A remarkable sequence of changes was found in axonal mitochondria of both unmyelinated and myelinated fibers. While these changes did not occur at precisely the same time in each fiber of

throughout the length of a single fiber, a temporal pattern of mitochondrial disruption was established. After 2–8 h exposure to a thallos salt, the size of axonal mitochondria was increased in comparison to controls. The normal small, cigar-shaped axonal mitochondria, seen in longitudinal sections of control tissue, were transformed into large, rounded structures containing many pleomorphic cristae and a granular matrix space (Figs. 9, 10). With time, the matrix space began to swell and clear, and the remaining cristae became shortened (Fig. 10). Although local fractures of the outer membrane were seen on occasion (Fig. 11), mitochondrial swelling was usually accompanied by loss of the inner membrane (Fig. 12).

After 24 h of exposure, axons contained numerous vacuoles, each possessing a few traces of mitochondrial cristae (Fig. 13). Frequently, adjacent to these vacuolated axonal mitochondria, an abnormal network of interlacing filamentous structures was detected. Individual strands, each measuring approximately 18 nm across, were in contact with both vacuolar membranes and with unidentified electron-opaque circular profiles in the axoplasm (Fig. 14).

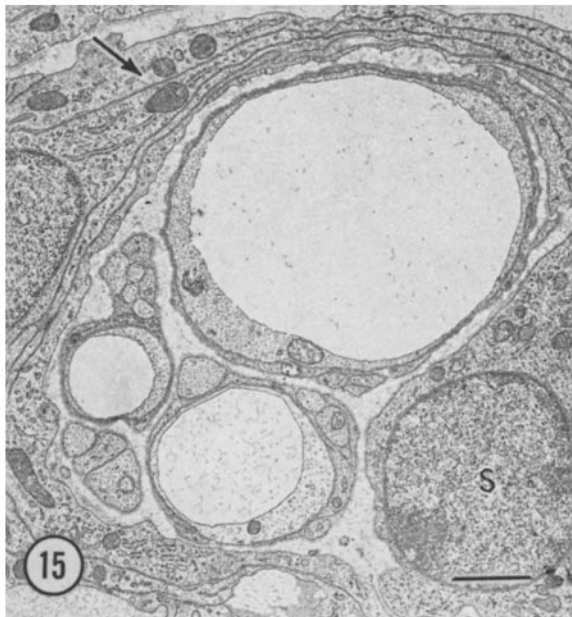
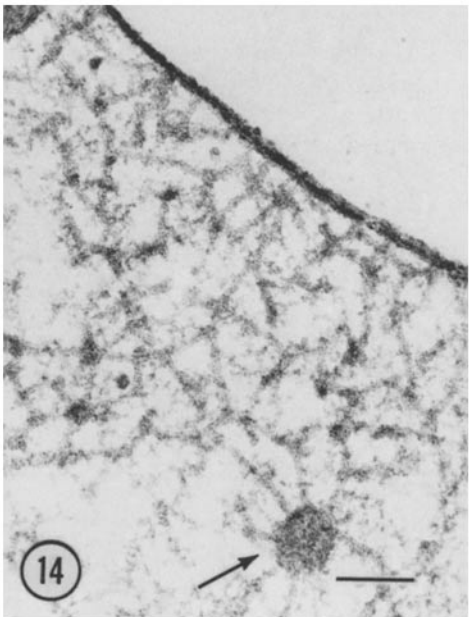
A longer exposure to thallos salts led to further swelling which caused adjacent vacuoles to abut (Figs. 15, 16). The trilaminar structure of the outer mitochondrial membrane surrounding each vacuole was preserved (Fig. 17), but the internal surface was frequently thickened and more electron opaque (Fig. 18). At points of contact, the trilaminar outer mitochondrial membrane of each of the two adjacent vacuoles fused to form a single pentalaminar membrane. Rupture of this mem-

FIGURE 9 A small cigar-shaped, largely normal, axonal mitochondrion from a longitudinally sectioned PNS fiber. Culture exposed to thallos sulfate for 2 h. Bar, 0.25 μm . $\times 50,000$.

FIGURE 10 After 24 h of exposure to a thallium salt, PNS axonal mitochondria are enlarged and are seen as rounded profiles in longitudinal section. The large mitochondrion on the left displays many pleomorphic cristae and a granular matrix space. In the mitochondrion on the right, the matrix space is swollen and clear, leaving a small axonal vacuole surrounded by both inner and outer mitochondrial membranes. Remnants of cristae are readily discernable. Bar, 0.5 μm . $\times 47,000$.

FIGURE 11 A mitochondrion from a PNS axon shows swelling with rupture of the outer mitochondrial membrane; free ends are marked by arrows. A portion of an adjacent axonal vacuole (V) is surrounded by a single trilaminar membrane with a similar density to the outer mitochondrial membrane. Bar, 0.1 μm . $\times 126,000$.

FIGURE 12 An axonal mitochondrion shows the partial disappearance of the inner mitochondrial membrane. Broken ends of a fragment of this membrane are indicated by arrows. Bar, 0.1 μm . $\times 102,000$.



brane led to fusion of juxtaposed vacuoles, thereby forming compartments which ultimately occupied the majority of the axon (Figs. 18, 19). Both swollen mitochondria and intra-axonal compartments were each surrounded by a trilaminar membrane which displayed an unusual electron density (Figs. 20, 21).

Finally, after several days' exposure to the thallium salt, the membrane surrounding each intra-axonal compartment often ruptured at multiple sites and the membrane fragments formed small ringlets. The remaining fluid-filled space, demarcated by the membrane fragments, did not merge with the surrounding axoplasm but persisted as a distinct entity within the distended axon (Fig. 23). The axolemma remained uninvolved although membrane imperfections were sometimes encountered at nodal regions. Neurotubules and neurofilaments were retained but haphazardly arranged. Increased numbers of axoplasmic dense membranous bodies were not encountered but particles resembling glycogen granules were prominent during the early hours of intoxication. Massive axonal vacuolation, occurring at and near nodes of Ranvier, appeared to cause retraction of myelin leaving portions of axons ensheathed only by Schwann cell cytoplasm (Figs. 3, 16). Schwann cells and their mitochondria were otherwise unchanged.

CNS fibers within the connected cord explant showed a less severe but otherwise identical series of changes in axonal mitochondria, leading to the formation of large unfused axonal vacuoles (Fig. 23). Swollen mitochondria were also seen in the axonal component of synaptic complexes. Neuronal perikaryal mitochondria were relatively less affected by exposure to thallosalts. Glial mitochondria remained unchanged (Fig. 24).

Only the distal portions of PNS motor fibers were examined by electron microscopy. Their axons displayed an identical sequence of mitochondrial swelling to that seen in dorsal root fibers. Terminal expansions of motor axons contained swollen mitochondria or vacuoles, but the structural integrity of the neuromuscular junction was unimpaired (Fig. 25). Muscle tissue rarely displayed mitochondrial vacuolation. Fibroblasts, comprising the PNS connective tissue, also contained structurally normal mitochondria.

ELECTRON MICROPROBE MASS SPECTROMETRY: Small K_{α} and $K_{\beta 1}$ peaks for thallium were detected in numerous cytoplasmic loci including areas where the axoplasm was replaced by contiguous vacuoles, each surrounded by an electron-opaque membrane. When portions of these membranes were examined in an EMMA 4 quantitative analytical electron microprobe analyzer, osmium was detected in much higher concentrations than thallium.

DISCUSSION

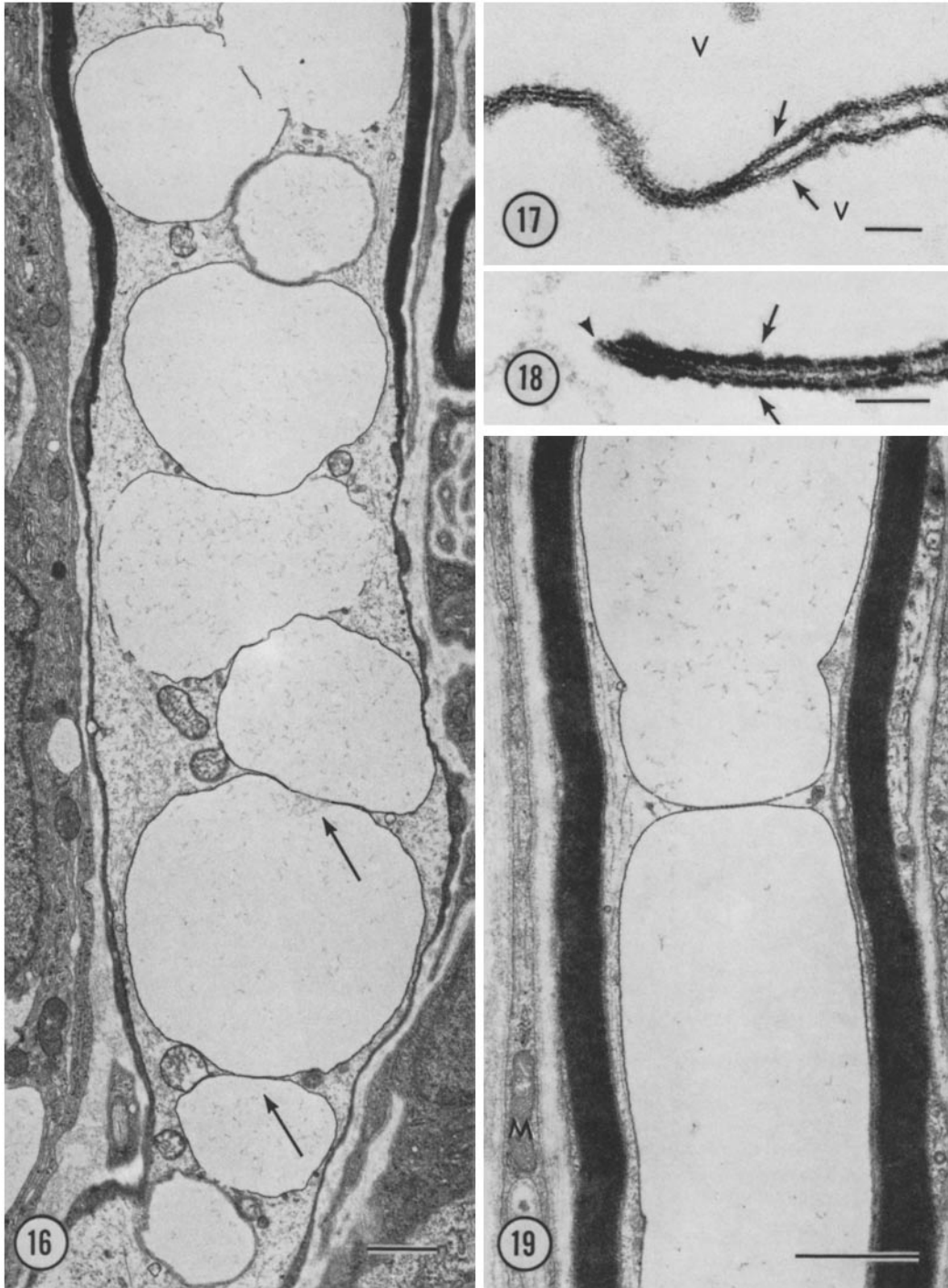
The present study has shown that thallosalt intoxication of CNS-PNS-muscle combination cultures produces nerve fiber swellings which are specifically axonal in origin, thus confirming the findings of a previous light microscope report on cultured PNS tissue similarly intoxicated (23, see also 35). In addition, our electron microscope observations demonstrate involvement of the entire length of both dorsal root and motor PNS fibers, CNS fibers, plus the axonal component of central and peripheral synaptic complexes.

The axonal vacuoles originated from enlarged mitochondria which underwent considerable swelling of their matrix spaces. These altered mitochondria became progressively swollen until

FIGURE 13 After 48 h of exposure to a thallium salt, PNS axons contain numerous vacuoles, each derived from a swollen mitochondrion (*M*). Smaller vacuoles are surrounded by both limiting mitochondrial membranes and contain remnants of cristae (arrowheads). Another vacuole (*V*), is in part surrounded by two membranes, while the largest vacuoles only possess one membrane, thought to be derived from the outer mitochondrial membrane. Unusual, interlacing, filamentous material is seen adjacent to an altered mitochondrion (arrow). Other axoplasmic elements are displaced. Bar, 0.5 μm . $\times 30,000$.

FIGURE 14 Interlacing filamentous material, similar to that seen adjacent to a mitochondrion in Fig. 13, is composed of strands approximately 18 nm across, some of which contact the vacuolar membrane and others which contact the dense circular structure in the axoplasm. Bar, 0.1 μm . $\times 98,000$.

FIGURE 15 Large axonal vacuoles are visible in cross-sectioned unmyelinated fibers. Mitochondria within Schwann (*S*) and connective tissue cells (arrow) are not swollen. 72 h of exposure to thallosalt. Bar, 1 μm . $\times 10,000$.



cristae and connected inner mitochondrial membranes were lost. In contrast to reports of the swelling behavior of isolated mitochondria (e.g., 36, 37), rupture and loss of the outer membrane did not appear to be the leading process. Contiguous vacuoles, each bounded by the remaining outer mitochondrial membrane, fused to form large compartments within an intact axolemma.

Specificity of Thallium for Axons

The ability of thallos salts to induce massive axonal changes may be related to the special properties of the axolemma. Nerve fibers contain large quantities of ATPase within the axolemma since this enzyme system is integral for proper intraxonal balance of water, sodium and potassium ions, and for recovery from impulse propagation. Inhibitors of plasma membrane ATPase, such as ouabain (38) and sodium azide (39), produce specific swelling of the Golgi apparatus and endoplasmic reticulum of dorsal root ganglion perikarya in vitro (40, 41). High external concentrations of thallos ions can inhibit plasma membrane ATPase (13). This may explain the findings of Hendleman (35) who, contrary to the present findings, reported a marked swelling of perikaryal granular endoplasmic reticulum when higher levels of thallos acetate (10^{-3} and 10^{-4} M) were exposed to cultures of rat dorsal root ganglia. However, if thallium had inactivated axolemmal ATPase in the present system, electrical stimulation would probably have failed to produce cord discharges and synchronized contraction of the muscle tissue. Normal electrophysiologic functioning

was maintained throughout the period of intoxication¹. Furthermore, the axolemma was not rendered electron opaque by deposition of thallium. These data suggest that inhibition of axolemmal ATPase did *not* play a leading role in the development of the selective axonal change. In other tissues, it has been found that the Tl^{+} possesses a high affinity for the K^{+} site of (Na^{+}, K^{+}) -activated ATPase (2, 4, 6, 10, 11) and may be actively transported across plasma membranes, in substitution for potassium ions, without inhibiting the enzyme system (2, 4, 8, 11). Active transport of Tl^{+} into axons, and its retention within the axoplasm, might have resulted in a temporal increase in the level of axoplasmic thallium.

Mechanisms of Mitochondrial Damage

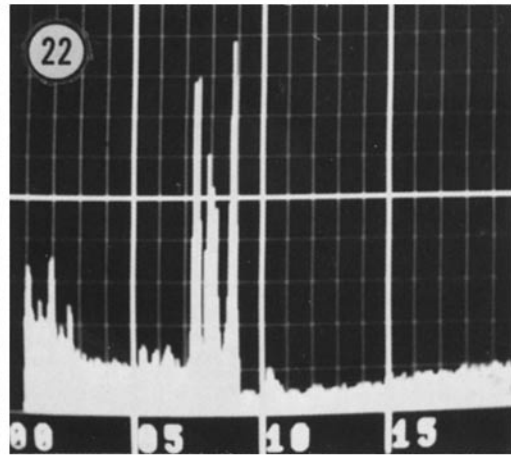
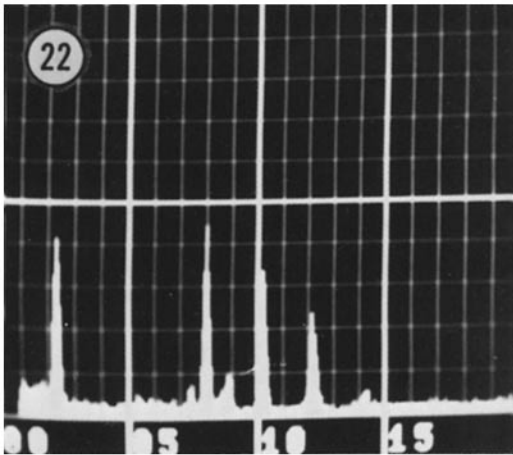
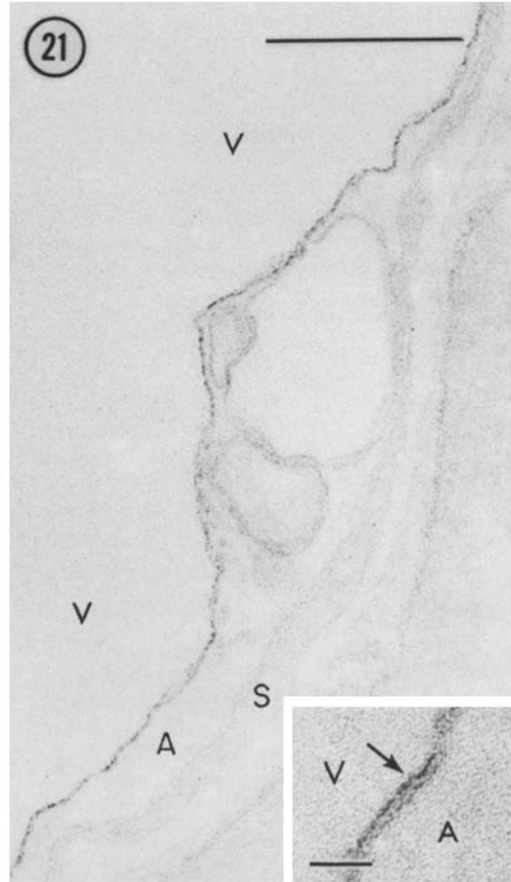
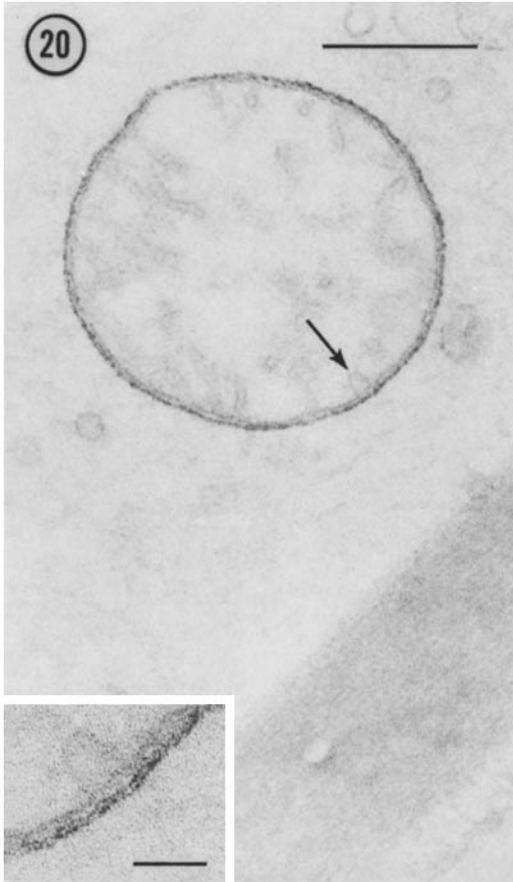
The leading cellular change induced by thallos salts was seen in axonal mitochondria which initially increased in size and subsequently underwent massive swelling. The mechanisms which are involved in the swelling of mitochondria are not fully understood. Swelling, i.e. water uptake, is usually associated with an accumulation of ions. Although this fact is consistent with a simple osmotic mechanism, the potential volume uptake appears to exceed that accountable for by osmotic forces alone. Sulfhydryl (SH) reagents unaccountably increase the permeability of isolated mitochondria, leading to water influx and swelling (42). Thallium is thought to be a SH reagent, capable of binding to SH groups of cystine precursors, causing a deficiency of cystine and a depletion of glutathione and of enzyme proteins, which are dependent upon cystine for their SH groups

FIGURE 16 A PNS fiber from a culture exposed to thallos sulfate for 48 h. The axon contains large numbers of contiguous vacuoles (cf. Fig. 3), each bounded by a single membrane (see Figs. 19, 20). The resultant fiber swelling has caused the myelin sheath, but not the Schwann cell cytoplasm, to retract from its normal paranodal position. Areas at arrows correspond to Figs. 17 and 18. Bar, $1 \mu m$. $\times 10,000$.

FIGURE 17 Where two adjacent axonal vacuoles (*V*) abut (lower arrow in Fig. 16), the two trilaminar vacuolar membranes (arrows) fuse to form a single pentalaminar membrane (left). Bar, 50 nm. $\times 150,000$.

FIGURE 18 A serial section taken from the area indicated by the upper arrow in Fig. 16. At the region of vacuolar coalescence, the fused pentalaminar membrane is broken (arrowhead). Note the enhanced density and increased thickness of the innermost leaflet (arrows) of each of the two apposed trilaminar vacuolar membranes. Bar, 50 nm. $\times 210,000$.

FIGURE 19 A PNS fiber is shown in which contiguous vacuoles have coalesced to form large, single membrane-bound, intra-axonal compartments. Axolemma, neurotubules, and neurofilaments remain. A Schwann cell mitochondrion (*M*) is unaffected. 48 h of exposure to thallos sulfate. Bar, $1 \mu m$. $\times 18,000$.



(16). Both cysteine and reduced glutathione induce swelling in isolated rat liver mitochondria (43). In view of these data and their own observations, Herman and Bensch suggested that thallium bound to mitochondrial membranes (19). Our observations on unstained sections examined by electron microscopy demonstrate an unusual density on both leaflets of outer mitochondrial membranes after exposure to thallium. Using electron microprobe mass spectrometry, it was possible to detect thallium in these membranes but considerably higher levels of osmium were also found. It is, therefore, not possible to rule out thallium binding to the outer mitochondrial membranes of mitochondria, but it does seem likely that the unusual densities were largely the result of an enhanced osmium deposition similar to that described by Peracchia and Robertson (44). Attempts to examine the density characteristics of tissue fixed in glutaraldehyde alone failed because the membrane in question was not preserved.

Previously suggested sites for thallium inactivation of mitochondrial proteins do not correlate well with an outer membrane locale. For example, Thyresson (45) was able to inhibit aerobic respiration in tissue slices of various organs including brain. By testing the metabolism of various substrates, he deduced that thallium inhibited the oxidation of metabolites in the Krebs cycle except succinic acid. The apparent similarity between the clinical and neuropathologic effect of thallium salt

intoxication and vitamin B deficiency in monkeys, raises the possibility of riboflavin inactivation by thallium (20). Riboflavin deficiency in mice causes considerable swelling of hepatocyte mitochondria which is reversed after restoration of normal riboflavin levels (46). The cytochrome oxidase inhibitor azide, N_3^- (47) which is actively accumulated by mitochondria (48), produces large membrane-bound axonal vacuoles when administered to nervous tissue in vitro (41). While these indirect data favor the interpretation that thallium exerts a toxic effect on the mitochondrial respiratory chain (see also 49), preliminary experiments employing isolated rat liver mitochondria have demonstrated a normal stimulation of mitochondrial respiration by valinomycin in the presence of thallium instead of potassium².

Pathologic Significance

It is uncertain how this study relates to the neurotoxicity of thallium in vivo, but the findings are in keeping with a sensitivity of the nerve cell and especially its axon to thallosalts. Retraction of myelin sheaths from nodes of Ranvier appeared to be a secondary phenomenon as the sheath compensated for the increase in axonal volume caused by the intra-axonal vacuoles. In man, thallium characteristically produces a distal, predominantly

² Spencer, P. S., W. Cammer, and C. Moore. Unpublished data.

FIGURE 20 An unstained section of a PNS fiber shows a swollen mitochondrion. Compare the density of the outer mitochondrial membrane with that of adjacent membranes including each crista (arrow) and the myelin sheath (lower right corner). Bar, 0.25 μm . *Inset* shows a portion of the mitochondrion (at arrow) which illustrates that the specific density is present on both leaflets of the outer membrane. 48 h of exposure to thallosulfate. Bar, 50 μm . $\times 77,000$. *Inset*, $\times 195,000$.

FIGURE 21 An unstained section shows an unmyelinated PNS fiber containing fused axonal vacuoles (V). Note the density of the vacuolar membrane relative to membranes surrounding the axon (A) and Schwann cell (S) which cannot be clearly discerned. Bar, 0.5 μm . *Inset* shows a portion of the same unstained vacuolar membrane. Note the trilaminar structure of this single membrane and its innermost leaflet which displays the greatest density (arrow). 48 h of exposure to thallosulfate. Bar, 25 nm. $\times 52,000$. *Inset*, $\times 280,000$.

FIGURE 22 Electron microprobe traces. Left, taken from a control sample of thallic oxide, displaying thallium peaks at 2.3, 10.3, 12.2, and 14.3 \AA . 100 s scan, 1,000 counts full scale. Right, taken from a swollen mitochondrion-axonal vacuole such as that illustrated in Fig. 20. Small K_{α} (2.3 \AA) and $K_{\beta 1}$ (10.3 \AA) peaks for thallium are visible as well as larger peaks for osmium ($K_{\alpha} = 1.9 \text{\AA}$) and sodium ($K_{\alpha} = 1.0 \text{\AA}$) from the fixative and buffer. The largest peaks correspond to copper and iron from the grid and microscope lenses, respectively. Spot size, 4.5 μm . 3,000 s scan, 1,000 counts full scale. Section thickness, approximately 50 nm.

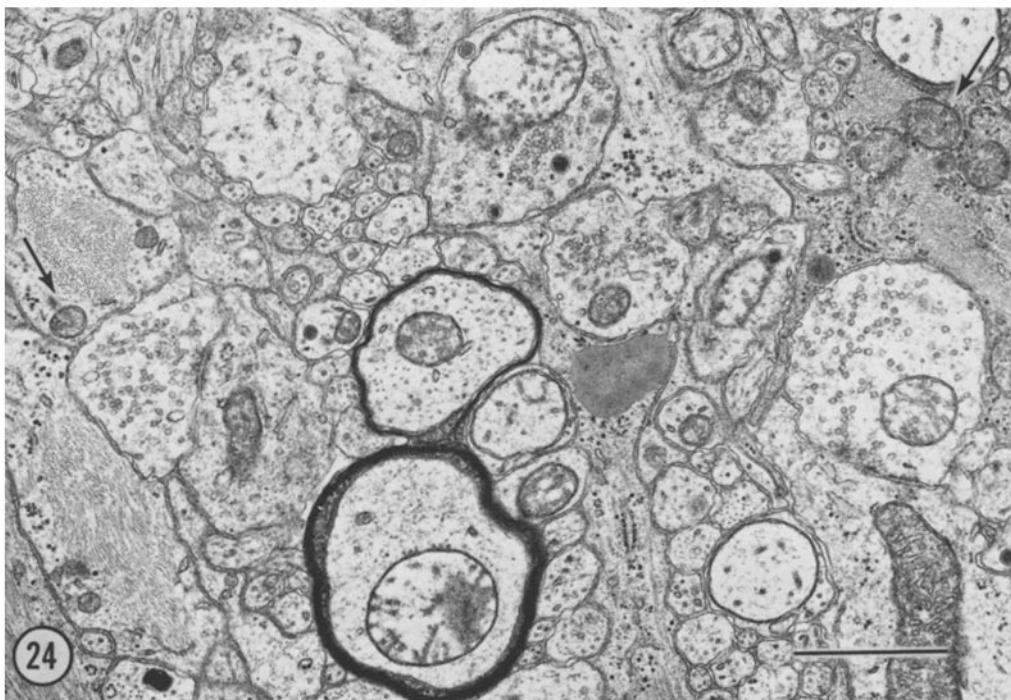
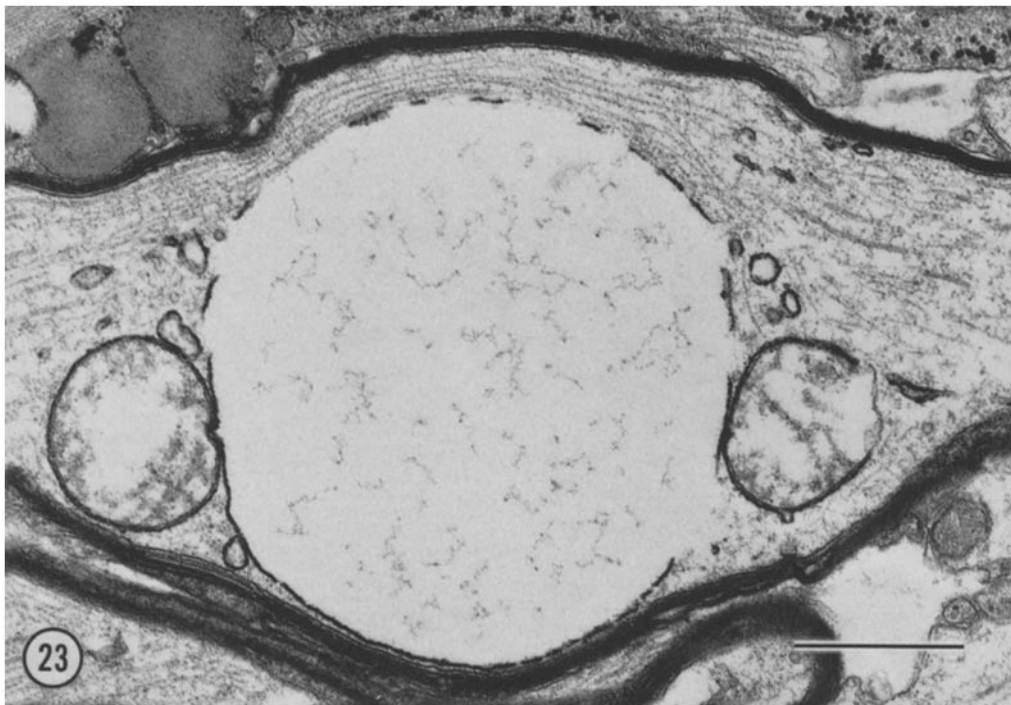


FIGURE 23 A myelinated CNS fiber, close to a node of Ranvier, contains swollen axonal mitochondria (left and right) and a large central vacuole which displaces the fiber laterally. Note that although the dense vacuolar membrane is disrupted at numerous loci, there is little evidence of mixing of axoplasm and vacuolar contents. 48 h of exposure to thallosulfate. Bar, $0.5 \mu\text{m}$. $\times 45,000$.

FIGURE 24 CNS tissue taken from the cord portion of a combination culture exposed to thallosulfate for 48 h. Swollen mitochondria are visible in myelinated and unmyelinated axons. Glial mitochondria are unswollen (arrows). Bar, $1 \mu\text{m}$. $\times 19,000$.



FIGURE 25 A neuromuscular junction, probably immature (see reference 26), taken from a combination culture exposed to thalious sulfate for 72 h. Compare the swollen mitochondrion (*M*) within the terminal axon with the unswollen mitochondria in the surrounding muscle tissue. Bar, 1 μ m. \times 20,000.

sensory neuropathy with some CNS involvement (17, 21, 50). The fine structural details of the underlying neuropathologic changes have not been defined although axonal involvement has been indicated³ (20, 51-53).

The present observation of a primary, specifically mitochondrial lesion within neurons exposed to thalious salts, illustrates only one facet of the enormous potential offered by the combination culture system in the study of neuromuscular biology. Not only does the system lend itself readily to the examination of numerous phenomena, but equally important, because the organotypic CNS-PNS-muscle tissue is functionally intact, the fundamental electrophysiologic applications, together with visual monitoring and electron microscopy, offer a new spectrum to the neuroscientist.

The authors thank Drs. Robert D. Terry and Murray B. Bornstein for their interest, advice, and support during the course of this study, and Dr. Stanley M.

³ Cavanagh, J. B. Personal communication.

Crain for his invaluable electrophysiologic data. The helpful discussion of Drs. Wendy Cammer, Boleslaw Liwnicz, and Cyril Moore is gratefully acknowledged. Technical assistance was kindly provided by Young Choi, Howard Finch, Miriam Pakingan, Everett Swanson, and Marianne Van Hooren. Philips Electronic Instruments (Mount Vernon, N. Y.), in collaboration with Edax International Inc. (Prairie View, Ill.), and AEI (England), generously performed the electron microprobe mass spectrometry.

Supported in part by grants NS 08952, NS 08770, NS 03356, and NS 06735 from the National Institutes of Health; grant 433-D-11 from the National Multiple Sclerosis Society; and a grant from the Alfred P. Sloan Foundation. Dr. Spencer is a postdoctoral fellow of a NIH Interdisciplinary Neurosciences Research Program (grant 5T1-MH-6418-16) and Dr. Raine is a NIH Research Career Development awardee, grant NS 70265. Dr. Madrid was a visiting WHO/PASB fellow from the Department of Neurology (Neuropathology), Hospital Salvador, Santiago-9, Chile.

Received for publication 18 December 1972, and in revised form 22 March 1973.

REFERENCES

1. KORENMAN, I. M. 1963. Analytical Chemistry of Thallium. Academy of Sciences of the USSR, translated by Israel program for scientific translations. Daniel Davey and Co. Inc., New York.
2. BRITTEN, J. S., and M. BLANK. 1968. Thallium activation of the (Na⁺-K⁺)-activated ATPase of rabbit kidney. *Biochim. Biophys. Acta.* 159:160.
3. DIAMOND, J. M., and E. M. WRIGHT. 1969. Biological membranes: the physical basis of ion and nonelectrolyte selectivity. *Ann. Rev. Phys.* 31:581.
4. KINSEY, E., I. W. MCLEAN, and J. PARKER. 1971. Studies on the crystalline lens. XVIII. Kinetics of thallium (Tl⁺) transport in relation to that of alkali metal cations. *Invest. Ophthalmol.* 10:932.
5. POTTS, A. M., and P. C. AU. 1971. Thallous ion and the eye. *Invest. Ophthalmol.* 10:12.
6. INTURRISI, C. E. 1969. Thallium-induced dephosphorylation of a phosphorylated intermediate of the (sodium + thallium-activated) ATPase. *Biochim. Biophys. Acta.* 178:630.
7. THYRESSON, N. 1951. Experimental investigation on thallium poisoning in the rat. *Acta Derm-Venerol.* 31:3.
8. MASLOVA, M. N., Y. V. NATOCHIN, and I. A. SKULSKY. 1971. Inhibition of active sodium transport and activation of Na⁺, K⁺-ATPase by ions Tl⁺ in frog skin. *Biokhimiya.* 36:867.
9. GEHRING, P. J., and P. B. HAMMOND. 1964. The uptake of thallium by rabbit erythrocytes. *J. Pharmacol. Exp. Ther.* 145:215.
10. GEHRING, P. J., and P. B. HAMMOND. 1967. The interrelationship between thallium and potassium in animals. *J. Pharmacol. Exp. Ther.* 155:187.
11. MULLINS, L. J., and R. D. MOORE. 1960. The movement of thallium ions in muscle. *J. Gen. Physiol.* 43:759.
12. RUSZNYÁK, I., L. GYÖRGY, S. ORMAI, and T. MILLNER. 1968. On some potassium-like qualities of the thallium ion. *Experientia (Basel).* 24:8.
13. KAYNE, F. J. 1971. Thallium (I) activation of pyruvate kinase. *Arch. Biochem. Biophys.* 143:232.
14. INTURRISI, C. E. 1969. Thallium activation of K⁺-activated phosphatases from beef brain. *Biochim. Biophys. Acta.* 173:567.
15. MUNCH, J. C., H. M. GINSBURG, and C. E. NIXON. 1933. The 1932 thallosis outbreak in California. *J. Am. Med. Assoc.* 100:1315.
16. GROSS, P., E. RUNNE, and J. W. WILSON. 1948. Studies on the effect of thallium poisoning of the rat. The influence of cystine and methionine on alopecia and survival periods. *J. Invest. Dermatol.* 10:119.
17. PRICK, J. J. G., W. G. SILLEVIS SMITT, and L. MULLER. 1955. Thallium poisoning. Elsevier Publishing Co., Amsterdam.
18. BASS, M. 1963. Thallium poisoning: a preliminary report. *J. Am. Osteopath. Assoc.* 63:229.
19. HERMAN, M. M., and K. G. BENSCH. 1967. Light and electron microscopic studies of acute and chronic thallium intoxication in rats. *Toxicol. Appl. Pharmacol.* 10:199.
20. PENTSHREW, A. 1971. Introduction to Intoxications. In Pathology of the Nervous System. J. Minckler, editor. McGraw-Hill, New York 2:1618.
21. BANK, W. J., D. E. PLEASURE, K. SUZUKI, M. NIGRO, and R. KATZ. 1972. Thallium poisoning. *Arch. Neurol.* 26:456.
22. WITHERS, A. R. 1972. Thallium poisoning in the dog. *Vet. Rec.* 90:1.
23. PETERSON, E. R., and M. R. MURRAY. 1965. Patterns of peripheral demyelination *in vitro*. *Ann. N. Y. Acad. Sci.* 122:39.
24. SPENCER, P. S., C. S. RAINE, and E. R. PETERSON. 1972. Effects of thallium on axonal mitochondria in cord-ganglion-muscle cultures. *J. Cell Biol.* 55:492A.
25. PETERSON, E. R., and S. M. CRAIN. 1972. Regeneration and innervation in cultures of adult mammalian skeletal muscle coupled with fetal rodent spinal cord. *Exp. Neurol.* 36:136.
26. PAPPAS, G. D., E. R. PETERSON, E. B. MASUROVSKY, and S. M. CRAIN. 1971. Electron microscopy of the *in vitro* development of mammalian motor end plates. *Ann. N. Y. Acad. Sci.* 183:33.
27. MASUROVSKY, E. B., and E. R. PETERSON. 1973. Photo-reconstituted collagen gel for tissue culture substrates. *Exp. Cell. Res.* 76:447.
28. CRAIN, S. M., L. ALFEI, and E. R. PETERSON. 1972. Neuromuscular transmission in cultures of adult human and rodent skeletal muscle after innervation *in vitro* by fetal spinal cord. *J. Neurobiol.* 1:471.
29. CRAIN, S. M., and E. R. PETERSON. 1967. Onset and development of functional interneuronal connections in explants of rat spinal cord-ganglia during maturation in culture. *Brain Res.* 6:750.
30. RAINE, C. S., L. A. FELDMAN, R. D. SHEPPARD, and M. B. BORNSTEIN. 1969. Ultrastructure of measles virus in cultures of hamster cerebellum. *J. Virol.* 4:169.
31. PETERSON, E. R., S. M. CRAIN, and M. R. MURRAY. 1965. Differentiation and prolonged maintenance of bioelectrically active spinal

- cord cultures (rat, chick and human). *Z. Zellforsch. Mikrosk. Anat.* 66:130.
32. BUNGE, M. B., R. P. BUNGE, and E. R. PETERSON. 1967. The onset of synapse formation in spinal cord cultures as studied by electron microscopy. *Brain Res.* 6:728.
 33. BUNGE, M. B., R. P. BUNGE, E. R. PETERSON, and M. R. MURRAY. 1967. A light and electron microscope study of long-term organized cultures of rat dorsal root ganglia. *J. Cell Biol.* 32:439.
 34. RAINE, C. S. 1973. Ultrastructural application of cultured nervous tissue to neuropathology. In *Progress in Neuropathology*. H. M. Zimmerman, editor. Grune and Stratton Inc., New York. 2:27.
 35. HENDLEMAN, W. 1969. The effect of thallium on peripheral nervous tissue in culture: a light and electron microscopic study. *Anat. Rec.* 163:198A.
 36. PARSONS, D. F., G. R. WILLIAMS, and B. CHANCE. 1966. Characteristics of isolated and purified preparations of the outer and inner membranes mitochondria. *Ann. N. Y. Acad. Sci.* 137:643.
 37. ERNSTER, L., and B. KUYLENSTIERNA. 1970. Outer membrane of mitochondria. In *Membranes of Mitochondria and Chloroplasts*. E. Racker, editor. Van Nostrand Reinhold Company, New York. 172.
 38. WESPI, H. H., D. MEVISSSEN, and R. W. STRAUB. 1969. The effect of ouabain and ouabagenin on active transport of sodium and potassium in vagus nerve fibres. *Arch. Int. Pharmacodyn. Ther.* 181:307.
 39. RICHTERLICH, R. 1958. Enzymopathologie. *Enzyme in Klinik und Forschung*. Springer-Verlag, Berlin. Quoted by Tischner and Murray (42).
 40. WHETSELL, W. O., and R. P. BUNGE. 1969. Reversible alterations in the Golgi complex of cultured neurons treated with an inhibitor of active Na and K transport. *J. Cell Biol.* 42:490.
 41. TISCHNER, K. H., and M. R. MURRAY. 1972. The effects of sodium azide on cultures of peripheral nervous system. *J. Neuropathol. Exp. Neurol.* 31:393.
 42. PRESSMAN, B. C. 1970. Energy-linked transport in mitochondria. In *Membranes of Mitochondria and Chloroplasts*. E. Racker, editor. Van Nostrand Reinhold Company, New York. 213.
 43. RILEY, M. V., and A. L. LEHNINGER. 1964. Changes in sulfhydryl groups of rat liver mitochondria during swelling and contraction. *J. Biol. Chem.* 239:2083.
 44. PERACCHIA, C., and J. D. ROBERTSON. 1971. Increase in osmiophilia of axonal membranes of crayfish as a result of electrical stimulation, asphyxia, or treatment with reducing agents. *J. Cell Biol.* 51:223.
 45. THYRESSON, N. 1950. Experimental investigation on thallium poisoning in the rat. *Acta Derm-Venerol.* 30:417.
 46. TANDLER, B., R. A. ERLANDSON, and E. L. WYNDER. 1968. Riboflavin and mouse hepatic cell structure and function. I. Ultrastructural alterations in simple deficiency. *Am. J. Pathol.* 52:69.
 47. KEILIN, D. 1936. The action of sodium azide on cellular respiration and on some catalytic oxidation reactions. *Proc. R. Soc. Lond. B Biol. Sci.* 121:165.
 48. PALMIERI, F., and M. KLINGENBERG. 1967. Inhibition of respiration under the control of azide uptake by mitochondria. *Eur. J. Biochem.* 1:439.
 49. MROZIKIEWICZ, A., and W. WIDY. 1964. Efficacité du cytochrome C dans l'empoisonnement expérimentale par le thallium. *Bull. Soc. Amis Sci. Poznan (Med.)*. 13:77.
 50. LE QUESNE, P. M. 1970. Iatrogenic neuropathies. In *Handbook of Clinical Neurology*. P. J. Vinken and G. W. Bruyn, editors. North-Holland Publishing Co., Amsterdam and American Elsevier Publishing Co., Inc., New York. 7(1):527.
 51. KARKOS, J. 1970. Pathomorphological changes in the nervous system and internal organs in poisoning with thallium compounds. *Pol. Tyg. Lek.* 25:1818.
 52. TACKMAN, W., and H. J. LEHMANN. 1971. Refraktarperiode und Serienimpulse im N. tibialis des Meerschweinchens bei akuter Thalliumpolyneuropathie. *Z. Neurol.* 199:105.
 53. OSETOWSKA, E. 1971. Metals. In *Pathology of the Nervous System*. J. Minckler, editor. McGraw-Hill Book Company, New York. 2:1647.